


ORIGINAL ARTICLE

Open Access



Computational modeling study of IL-15-NGR peptide fusion protein: a targeted therapeutics for hepatocellular carcinoma

Tehreem Fatima¹, Mian Muhammad Mubasher², Hafiz Muhammad Rehman^{1,3*}, Sakina Niyazi⁴, Abdullah R. Alanzi⁵, Maria Kalsoom¹, Sania Khalid¹ and Hamid Bashir^{1*} 

Abstract

The primary challenge to improving existing cancer treatment is to develop drugs that specifically target tumor cell. NGR peptide is tumor homing peptide that selectively target cancer cells while interleukin 15 is a pleiotropic cytokine with anticancer properties. This study computationally engineered a IL15-NGR fusion peptide by linking the homing peptide NGR with the targeting peptide IL-15. After evaluating and validating the chimeric peptide, we docked it to the IL-15R α /IL-15R β / γ c heterodimer receptor, examining the interactions and binding energy and lastly, molecular dynamics simulations were performed. The secondary and tertiary structures, along with physicochemical properties of the designed IL-15-NGR chimeric protein, were predicted using GOR IV, trRosetta and ProtParam online servers respectively. The quality and 3D structure validation were confirmed via ProSA-web and SAVES 6.0 analysis which predicted an ERRAT score of 96.72%, with 97.6% of residues in the Ramachandran plot, validating its structure. Finally, Docking, MD simulations and interaction analysis were performed using ClusPro 2.0 and GROMACS and PDBsum, which exhibited significant hydrogen bonding and salt bridges, confirming the formation of a stable docked complex. These results were further corroborated by simulation analysis, which demonstrated a stable and dynamic behavior of the docked complex in a biological environment. The predicted high expression value of fusion protein was 0.844 in *E.coli* using SOLUPROT tool. These findings suggest efficient expression of the IL15-NGR fusion protein if its gene is inserted into *E. coli* and indicates its potential as a safe and effective anticancer treatment, paving the way for targeted therapeutic interventions.

Introduction

By 2040, the World Health Organization predicts 28.9 million new cancer cases and 16.2 million deaths annually, highlighting the critical need for global action in prevention, detection, and treatment strategies (Jallow et al. 2022). Hepatocellular carcinoma, the primary liver cancer most frequently diagnosed globally, ranks as the second leading cause of cancer-related deaths (Siracusano et al. 2020). Hepatocellular carcinoma's varied risk factors and etiology contribute to its complex disease heterogeneity, posing challenges in diagnosis and treatment strategies worldwide (Liang et al. 2018). Over the

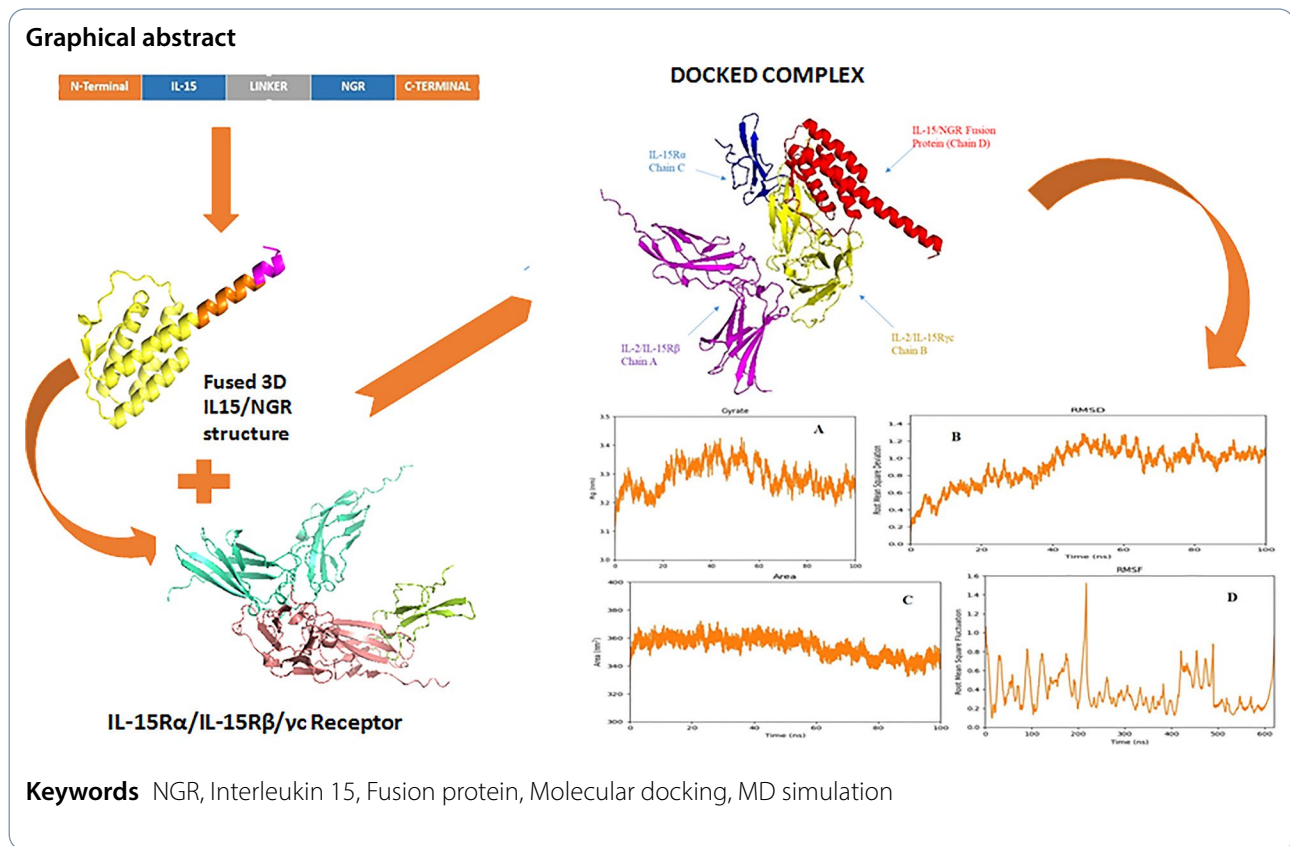
*Correspondence:

Hafiz Muhammad Rehman
muhammad.rehman@mlt.uol.edu.pk
Hamid Bashir
hamid.camb@pu.edu.pk

Full list of author information is available at the end of the article



© The Author(s) 2024. **Open Access** This article is licensed under a Creative Commons Attribution-NonCommercial-NoDerivatives 4.0 International License, which permits any non-commercial use, sharing, distribution and reproduction in any medium or format, as long as you give appropriate credit to the original author(s) and the source, provide a link to the Creative Commons licence, and indicate if you modified the licensed material. You do not have permission under this licence to share adapted material derived from this article or parts of it. The images or other third party material in this article are included in the article's Creative Commons licence, unless indicated otherwise in a credit line to the material. If material is not included in the article's Creative Commons licence and your intended use is not permitted by statutory regulation or exceeds the permitted use, you will need to obtain permission directly from the copyright holder. To view a copy of this licence, visit <http://creativecommons.org/licenses/by-nc-nd/4.0/>.



last decade, advancements in hepatocellular carcinoma prevention, diagnosis, and therapy have been notable, emphasizing risk factor avoidance to potentially decrease incidence. However, conventional treatments face limitations due to tumor size and intra-hepatic metastases, constraining surgical and other therapeutic interventions (de Lope et al. 2012). Cancer chemotherapy induces tumor cell death while potentially stimulating antitumor immunity through mechanisms like “immunogenic cell death” and reduction of immunosuppressive cells within the tumor microenvironment (REHMAN et al. 2023). While chemotherapy can induce tumor cell death and contribute to antitumor immunity, it may not prevent the development of drug resistance genes in certain individuals (Le Grazie et al. 2017). The liver’s immunosuppressive microenvironment and the absence of unique tumor-associated antigens in hepatocellular carcinoma limit the efficacy of existing therapies, necessitating the development of more potent approaches. Recent research suggests that immunotherapy could offer a promising therapeutic avenue for hepatocellular carcinoma patients, potentially addressing these challenges and improving treatment outcomes (Breous and Thimme 2011). Certain tumors have exhibited favorable responses to immunotherapy through oral administration of cytokines, which stimulate immune responses (Aslam et al. 2023). In

addition to IL-21, IL-7, IL-6, IL-3, IL-2, GM-CSF (granulocyte-macrophage colony stimulating factor) and G-CSF (granulocyte-colony stimulating factor), IL-15 belongs to 4 alpha helix bundle family of cytokines (Burton et al. 1994). High levels of IL-15 mRNA expression are found in monocytes, skeletal muscle, thymus, bone marrow stroma, heart, macrophages, lung, liver, thymic epithelium, kidney, and placenta. It is a multifunctional cytokine that plays a crucial role in the formation, activation, survival of immune effector cells, homing, and particularly CD8⁺T cells and natural killer (NK), contributing significantly to immune system function and response (Alpdogan and van den Brink 2005). Interleukin-15 (IL-15) has emerged as a promising immunotherapeutic agent for both hematological malignancies and solid tumors due to its potent immunostimulatory properties (Leonard et al. 2019; Shourian et al. 2019). As a member of the common gamma chain (γ c) receptor family, IL-15 shares signaling pathways with cytokines like IL-2 and IL-4 but distinguishes itself by acting as a critical signaling molecule in the immunological synapse (Dubois et al. 2002). Administering IL-15 through continuous intravenous infusion at a dose of 20 mg/kg per day for 10 days resulted in a 7-fold increase in the number of circulating NK cells and an astounding 80- to 100-fold increase in the number of circulating effector memory T

cells (Sneller et al. 2011). Unlike IL-2, IL-15 administration significantly enhances NK cell activity, upregulates NKG2D receptor signaling (Decot et al. 2010; Zhang et al. 2008), and promotes the development and survival of CD8+ cytotoxic T lymphocytes, crucial for long-term anti-tumor immunity, without inducing regulatory T cell expansion, thereby preserving immune effector function and reducing toxicity (Munger et al. 1995; Sneller et al. 2011; Waldmann et al. 2011). Furthermore, IL-15 prevents activation-induced cell death (AICD) and shows potential in targeting cancer stem cells, making it a superior candidate for cancer immunotherapy (Marks-Konczalik et al. 2000).

Liver-targeted gene delivery of IL-15 significantly enhances the immune response against hepatocellular carcinoma (HCC) by expanding CD8+ T cells and NK cells, with a particularly prolonged accumulation of CD8+ T cells in the liver lasting over 40 days. This targeted IL-15 treatment has demonstrated remarkable therapeutic effects on both well-established liver metastatic tumors and DEN-induced autochthonous HCC, underscoring its potential as an effective treatment for liver cancer. The therapeutic benefits of IL-15 were specifically attributed to the presence of CD8+ T cells, as their depletion nullified the treatment effects, whereas NK cell depletion did not. This highlights the crucial role of CD8+ T cells in mediating IL-15's anti-tumor activity (Cheng et al. 2014).

When IL-15 binds to a heterodimer receptor composed of γ c chain along with IL-15R α , IL-2R β , it triggers signaling pathways that involve STAT (signal transducer and activator of transcription) molecules and Janus kinase (Jak). This activation cascade involves in mediating the cellular responses to IL-15, including proliferation, differentiation, and survival of immune cells such as CD8+ T cells and natural killer cells (Grabstein et al. 1994; Giri et al. 1995). The Asn-Gly-Arg (NGR) peptide interacts with the APN/CD13 (aminopeptidase N receptor) and this receptor frequently upregulated on the cellular membranes of endothelial cancer cells. This high tumor selectivity enables the NGR peptide to enhance drug delivery when conjugated with therapeutic proteins, resulting in lower toxicity compared to the administration of the drug alone (Arap et al. 1998). The tumor-homing property of the NGR peptide enables the direct delivery of therapeutic drugs to the targeted site, facilitating their internalization into tumor cells and passage through tumor vasculature (Wang et al. 2012). The NGR peptide demonstrates selective affinity for CD13, a transmembrane protein that is overexpressed on liver tumor cells and neovasculature, making it a valuable tool for targeted cancer therapy (Wang et al. 2012). By conjugating therapeutics with NGR peptides, these compounds can be specifically delivered to tumors, enhancing their

effectiveness while minimizing off-target effects. The CNGRC domain within the NGR peptide acts as a precise targeting moiety, directing conjugated therapeutics to the tumor vasculature and facilitating their penetration into the tumor. This targeted delivery system has shown promise in tumor and angiogenesis imaging as well. For instance, studies involving NGR-peptide conjugates like Oregon Green (OG) have demonstrated efficient cellular uptake at body temperature (37 °C) and enabled the targeted visualization of tumors through fluorescence imaging, highlighting the peptide's potential in cancer targeting and diagnostics (Negussie et al. 2010). The NGR peptide demonstrates exceptional selectivity for HepG2 tumor cells, minimizing off-target effects on healthy tissues. This targeted approach, coupled with its broad-spectrum efficacy against various cancers, positions the NGR peptide as a promising therapeutic strategy (Ng and Lee 2020).

The fusion of anti-cancer cytokines with tumor-homing peptides offers a promising therapeutic strategy for selectively targeting and treating cancerous cells. By leveraging the specificity of tumor-homing peptides, coupled with the cytotoxic effects of anti-cancer cytokines, this approach enhances the precision and effectiveness of cancer therapy while minimizing damage to healthy tissues. In this study, we aimed to theoretically design a bifunctional peptide comprising a targeting domain and a tumor homing domain. Specifically, we computationally joined the homing peptide NGR with the targeting peptide IL-15 to design a IL15-NGR fusion peptide. The design principle involved the selection of a rigid linker to fuse IL-15 and NGR, ensuring proper spatial orientation and functionality of both peptides. The rigid linker was chosen to maintain a certain distance between the functional domains of both peptides, allowing them to perform their functions independently without steric hindrance. Subsequently after quality assessment and validation of chimeric peptide, we docked this peptide to the heterodimer receptor (IL-15R α /IL-15R β / γ c) and analyzed the interactions and binding energy. Finally, molecular dynamics simulation was conducted on the docked complex to predict its stability, compactness, and behavior in a biological environment.

Materials and methods

Construction of IL-15/NGR chimeric protein

The mature peptide amino acid sequence of Interleukin 15 was retrieved with (accession no AF031167.1) from NCBI Database (<https://www.ncbi.nlm.nih.gov/>). The FASTA amino acid sequence of NGR (tumor homing peptide) was obtained from previously published data (Lei et al. 2010) and retrieved from NCBI Database. In order to construct the chimeric protein the mature peptide of IL-15 was fused with NGR peptide at C terminal

via a rigid linker. Table 1 shows FASTA sequence of fusion protein.

Prediction of secondary structure of designed fusion protein

The FASTA amino acid sequence of newly constructed fusion protein was submitted in GOR IV (https://npsabpibil.ibcp.fr/cgi-bin/npsa_automat.pl?page=/NPSA/npsa_gor4.html) which can predict the secondary structure of chimeric protein (Sen et al. 2005). We access the functional features such low complexity sections, solvent accessibility surface area coiled-coil domain, secondary structure, and disulphide bond position as described (Rezaie et al. 2020). The total number of beta sheets and alpha helix in constructed fusion protein were also be predicted via online server.

Homology modelling of the chimeric IL-15- NGR protein

In order to predict a reliable 3D model (three-dimensional structure) of IL-15- NGR fusion protein, the primary sequence of protein submitted to I-TASSER online server (<https://zhanggroup.org/I-TASSER/>) and trRosetta (<https://yanglab.qd.sdu.edu.cn/trRosetta/>). The structure validation and quality assessment of constructed 3D models were evaluated by using different online software such as ERRAT2 (<https://saves.mbi.ucla.edu/>), that can predict the overall quality factor, ProSA-web server for z-score assessment along with local quality estimate and finally Rampage online (<https://saves.mbi.ucla.edu/results?job=1553129&p=procheck>) server was used which constructed a Ramachandran plot through PROCHECK for structure validation (Pourhadi et al. 2019).

The physiochemical features of the chimeric IL-15/NGR protein

ProtParam tool online server (<https://web.expasy.org/protparam/>) was used for analyzing physiochemical properties including aliphatic index, molecular weight, half-life, grand average of hydropathicity (GRAVY), isoelectric point and amino acid composition of chimeric IL-15-NGR protein (Gasteiger et al. 2005). The solubility of designed chimeric IL-15-NGR fusion protein was

predicted by using Protein-sol (<https://protein-sol.manchester.ac.uk/>) online server (Hebditch et al. 2017).

Assessment of toxicity, allergenicity, and antigenicity

To evaluate the allergic, antigenic, and toxic properties of the chimeric protein, its amino acid sequence was subjected to analysis using three web servers: AlgPred, VaxiJen, and Toxinpred. AlgPred2, a tool for predicting allergenicity, was employed to identify regions within the protein sequence that correspond to known epitopes. VaxiJen, on the other hand, determined antigenicity based on the chemical and physical characteristics of the protein. A threshold value of 0.5 was utilized to distinguish between antigenic and non-antigenic properties. Lastly, the Toxinpred server was utilized to predict potentially toxic amino acid regions in the chimeric protein sequence.

Molecular docking and protein-ligand interaction

The docking of the IL-15-NGR fusion protein with the IL15R α /IL15R β / γ c receptor was performed using two different software tools, Hdock and ClusPro 2.0, to compare and validate the docking results. By utilizing both platforms, we aimed to ensure the reliability and consistency of the docking predictions. This comparative analysis allowed us to cross-verify the interaction patterns and binding energies obtained from each tool, thereby increasing confidence in the accuracy of our findings. For docking purpose tertiary structure of IL15R α β receptor was downloaded from Protein Data Bank with PDB ID: 4GS7. Prior proceeding to docking, Pymol (<https://pymol.org/2/>) tool was used for removing the impurities (water molecule and ligands) and attached IL15 molecule present in PDB structure of the IL15R α β receptor molecule. The protein-protein interactions of the obtained docked complex were analyzed on PDBsum server, the server provide the information of complex such as interacting interfaces, hydrogen bonds, nonbonded contacts, pores, salt bridges and tunnels (Laskowski 2009). Finally, the binding affinity and binding energy of the docked complex was calculated using the PRODIGY (Vangone and Bonvin 2015) and HawkDock (Chen et al. 2016) online servers.

Soluble expression prediction in *Escherichia coli*

For predicting the soluble protein expression level in *Escherichia coli*, SoluProt bioinformatics tool was used. A bioinformatics tool called SoluProt is used to predict the production of soluble proteins in *E. coli* on the basis of sequence. The tool predicts the expressibility and solubility of the proteins under study concurrently (Hon et al. 2021) (Ghomi et al. 2020).

Table 1 Primary sequence of IL-15/NGR fusion protein

Peptide	FASTA Sequence	Amino acids no.	References
IL-15	NWVNVISDLKKIEDLIQSMHIDATLYTES-DVHPSCKVTAMKCFLELQVISLESGDA-SIHDTVENLILANNLSSNGNVTESGCK-ECEELEKNIKEFLQSFVHIVQMFINTS	342	NCBI accession no AF031167.1
Linker	AEAAAKEAAAKA	12	Zhao et al. (2008)
NGR	CNGRCGG	7	Lei et al. (2010)

Molecular dynamic simulation studies

The chimeric protein in complex with its receptor was studied for MD simulations by using GROMACS version 2022.4. The CHARMM36 jul-2021 force field (Vanommeslaeghe et al. 2010) and the standard TIP3P water model (Izadi et al. 2014) were chosen for MD simulations. A complex was embedded in the center of a cubic water box with a minimum distance from the complex to the box boundary of 10 Å. The complex was solved with water modeled by the TIP3P force field. The system was further neutralized by proper NaCl solution. Energy minimization was carried out for each complex using a steepest-descent integrator to reach negative potential energy and the maximum force for less than 1,000 kJ/mol/nm on any atom (Helal et al. 2022). To relax the protein complex, the equilibration was performed with positional restraints on all heavy atoms of complex under two ensembles, NVT (constant number of particles, volume and temperature) under constant temperature at 300 K for 100 picoseconds (ps), and NPT (constant number of particles, pressure, temperature) under constant pressure at 1 bar for 100 ps and trajectories were saved every 2 fs time step (Golo and Shaïtan 2002). The MD simulation was then performed for 100 ns. Changes in the track during simulation were evaluated and analyzed using following parameters: root mean square deviation (RMSD), root mean square fluctuation (RMSF), radius of gyration (Rg) and solvent accessible surface area (SASA).

Results

Construction of IL15-NGR chimeric protein

In order to construct a chimeric IL-15-NGR protein, amino acid sequence of IL15 and NGR was retrieved from the from NCBI database. Both the sequence were fused through the rigid linker that results in a chimeric protein with a single chain of 133 Amino acids (Fig. 1). A rigid linker was used to ensure the cleavage of fusion protein in two functional peptides and to prevent the disulphide bridge formation between peptides.

Secondary structure prediction

The amino acid sequence dictates the shape, structure, and function of a protein. GOR IV analysis predicted the secondary structure of the submitted chimeric protein, specifying the distribution of alpha helices and beta sheets. The predicted structure unveiled that the construct comprises 50.38% (67 residues) organized into alpha helices, 12.03% (16 residues) forming extended strands, and 37.59% (50 residues) adopting random coil

conformations (Fig. 2). The higher percentage of alpha helix in chimeric construct ensures structural stability of IL15-NGR (Sakurai et al. 2005).

Evaluation of tertiary structure of chimeric IL-15-NGR protein

Tertiary structure of designed chimeric protein was predicted by homology modeling using I-TASSER and trRosetta online servers. The top 5 models predicted by both servers were evaluated for selecting the most accurate configuration of designed chimeric protein on the basis of highest C-score and TM-score. The finalized model among I-TASSER was having C-score -1.50 and TM-score 0.53 ± 0.15 while the finalized model from trRosetta was having TM-score of 0.915. The selected most stable models were evaluated further for making comparison among the models predicted by two softwares I-TASSER and trRosetta.

Suitable 3D structure selection, validation, and quality assessment

To determine the stereochemistry of designed chimeric protein, the final IL15-NGR 3D structure obtained from I-TASSER and trRosetta was uploaded on SAVES online server. The most reliable structure among the two selected models from different softwares (I-TASSER and trRosetta) was selected on the basis of Verify 3D, Ramachandran plot and ERRAT value (Table 2).

The results indicate that the most stable and reliable structure was predicted by trRosetta (as shown in Fig. 3) that shows 97.6% residues in most favored region and ERRAT value of 96.72 as shown in Fig. 4B. Through GalaxyRefine tool, trRosetta predicted IL15-NGR 3D structure was refined and validated by Ramachandran plot, ERRAT analysis. Ramachandran plot analysis was done by PROCHECK which shows that the IL15-NGR model contains 99 residues in Ramachandran most favored region (Fig. 4A). For analyzing the non-bonded interactions statistics among various atom types IL15-NGR 3D structure was uploaded on ERRAT program. Higher ERRAT value indicates high quality of 3D structure. ERRAT value of final model was predicted to be 96.72 (Fig. 4C).

Figure 5A illustrates the model quality, with black dots representing the IL-15/NGR fusion protein's data points. These dots, situated among dense clusters of X-ray and NMR data, signify a negative Z-score of -6.2 which is consistent with high-quality structures, affirming the fusion protein's reliable folding. The broad distribution of data points justify structural variability, yet the fusion protein's proximity to these clusters reinforces confidence in its computationally generated model. In Fig. 5B, the energy profile graph from ProSA-web for the IL-15/NGR fusion protein indicates predominantly negative values



Fig. 1 Schematic representation of IL-15 fusion with NGR



Fig. 2 Secondary structure prediction of IL-15/NGR via GOR IV

Table 2 Comparison of the quality of 3D models predicted by different software

3D model generated on	Percentage residues in most favored RC region	ERRAT quality score
I-TASSER	79.2	89.6
trRosetta	97.6	96.72

across most sequence positions, suggesting structural stability. Fluctuations, particularly with a smaller window size, reveal localized variations in stability, smoothed out in larger window sizes, implying overall structural integrity.

Prediction of the physiochemical properties of chimeric protein

Using the ProtParam web service, the physical and chemical characteristics of the protein were estimated after submitting amino acid sequence. Table 3 summarized all the Parameters of chimeric protein. The chimeric protein has calculated theoretical PI value 4.89 and estimated molecular weight 14503.49. The ratio of negatively charged residues (Asp+Glu) in chimeric protein is 19 and positively charged residues (Arg+lys) in chimeric protein is 11, this imparts that this chimeric protein (IL-15/NGR) has Acidic properties. For protein-protein interaction studies, the extinction coefficient value of chimeric protein plays a very important role. The estimated half-life of chimeric protein in vitro among mammalian reticulocytes is 1.4 h and in E.coli the estimated half-life

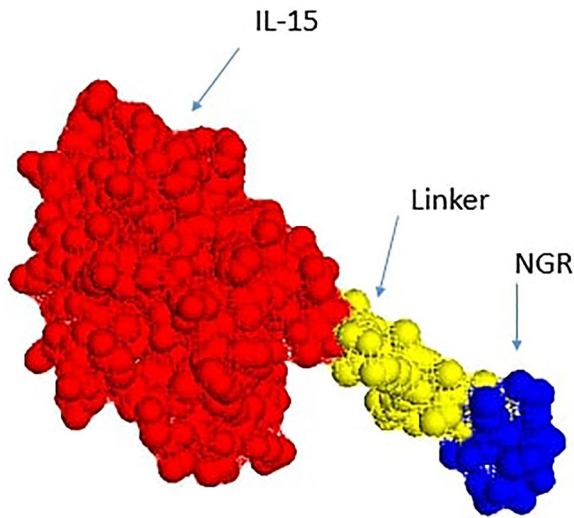


Fig. 3 PYMOL illustration of IL-15/NGR fusion protein

is more than 10 h. The value of instability index estimated is 50.38 and aliphatic index value is 96.09 which indicates the protein stability over wide range of temperature. The value of gravity index indicates the reactivity of chimeric protein. The Protparam server generated -0.047 GRAVY value of chimeric protein. This fusion protein's extremely low GRAVY index suggests that IL-15 NGR may lead to a more effective interaction with water.

Solubility prediction in chimeric protein

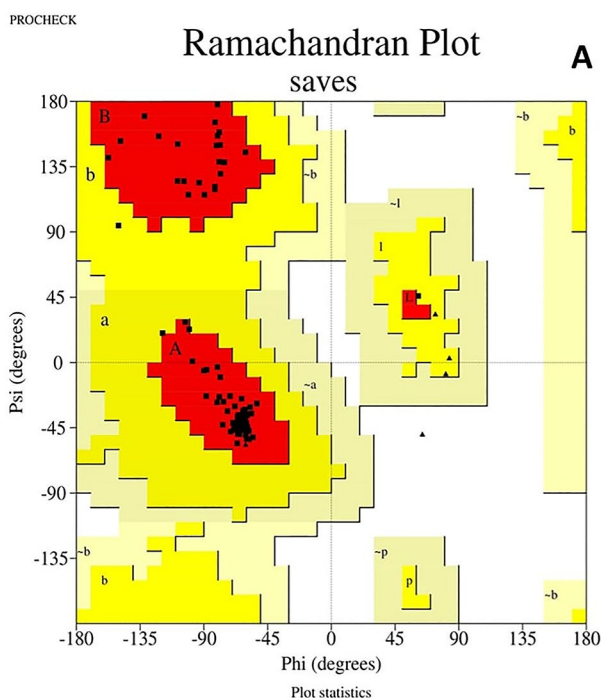
The FASTA amino acid sequence was processed using the protein-sol programme in order to evaluate soluble expression of fusion protein in *E.coli*. The prosol web server determines the solubility of proteins by contrasting the average solubility of the population dataset in *E. coli* with the anticipated solubility of the query sequence (Hebditch et al. 2017). The threshold value for protein solubility set by protein-sol server is 0.45. As value of predicted chimeric protein is 0.844 (Fig. 5C) which is greater than threshold value, this indicates that designed protein is highly soluble. The PI value of the designed protein is 4.880.

Evaluation of toxicology, allergenicity, and antigenicity

According to predictions made by Toxinpred, Algpred Vaxigen servers, Algpred, Vaxigen servers, the engineered chimeric protein IL-15-NGR is nontoxic. The protective antigen score was 0.5 overall. The finding imply that chimeric protein is non-immunogenic and can be used as a promising therapeutic target for cancer.

Docking analysis

In order to predict interaction between designed chimeric protein and its IL-15R α /IL-15R β / γ c receptor, molecular docking was performed by using the Cluspro online server. ClusPro operates on the Fast Fourier Transform Correlation technique, it assess the docked complexes in three stages. First, the rigid docking is carried out by



Plot statistics	
Residues in most favoured regions [A,B,L]	B 122 97.6%
Residues in additional allowed regions [a,b,l,p]	3 2.4%
Residues in generously allowed regions [-a,-b,-l,-p]	0 0.0%
Residues in disallowed regions	0 0.0%

Number of non-glycine and non-proline residues	125 100.0%
Number of end-residues (excl. Gly and Pro)	1
Number of glycine residues (shown as triangles)	6
Number of proline residues	1

Total number of residues	133

Based on an analysis of 118 structures of resolution of at least 2.0 Angstroms and R-factor no greater than 20%, a good quality model would be expected to have over 90% in the most favoured regions.

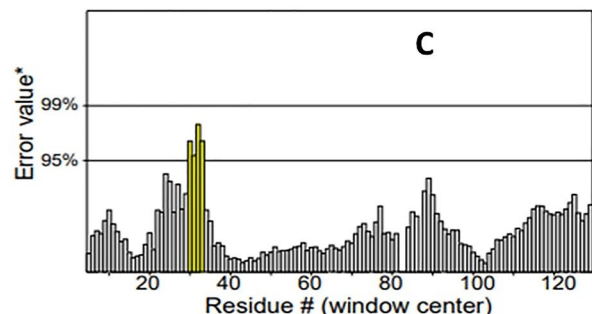


Fig. 4 Structure validation and quality index of IL15-NGR fusion protein

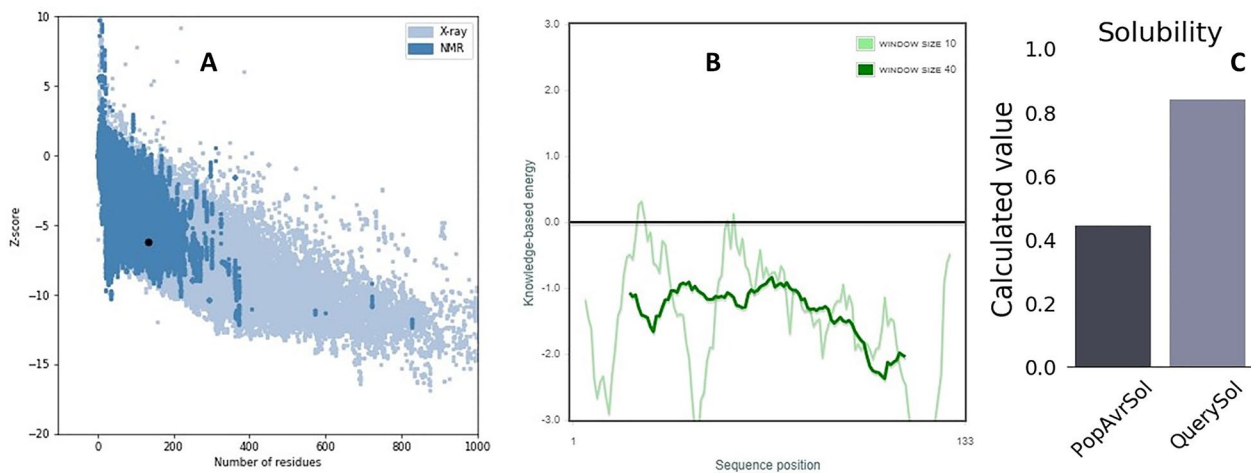


Fig. 5 Quality assessment graphs and solubility prediction of IL-15/NGR fusion protein

Table 3 Physicochemical properties of IL15-NGR fusion peptide

Physicochemical parameters	Values
Total No of amino acids	133
Theoretical PI value	4.89
Total negatively charged amino acid residues	19
Total positively charged amino acid residues	11
Extinction coefficient value	7365 M ⁻¹ cm ⁻¹
GRAVY	-0.047
Stability prediction	53.38
Aliphatic index value	96.09

Table 4 Cluster score of docked complexes

Cluster	Members	Representative	Weighted score
0	189	Center	-617.2
		Lowest energy	-801.0
1	58	Center	-676.0
		Lowest energy	-729
2	53	Center	-815
		Lowest energy	-833
3	44	Center	-633.9
		Lowest energy	-659.3
4	40	Center	-633.6
		Lowest energy	-675.0
5	39	Center	-637.5
		Lowest energy	-710.5
6	37	Center	-609.1
		Lowest energy	-663.0
7	36	Center	-694.9
		Lowest energy	-694.9
8	30	Center	-706.8
		Lowest energy	-706.8
9	30	Center	-681.8
		Lowest energy	-681.8
10	28	Center	-662.0
		Lowest energy	-662.0

analysing the conformations in billions with the aid of PIPER. Second, it predicts the biggest cluster and displays the most probable docked complex by creating clusters of one thousand lowest energy structures based on RMSD (root mean square deviation). The third stage involves energy reduction to stabilise the chosen docked model (Kozakov et al. 2017). Among 10 models generated by ClusPro server (Table 4), the selection of the best structure for protein-protein interaction studies was guided by factors such as model scores, electrostatic energies, and van der Waals attraction as described previously (Muhammad Rehman et al. 2023). Cluster 0 stands out with 189 members, the highest among all clusters, indicating a robust and consistent set of docking poses that suggest a reliable interaction model. The weighted score of -617.2 and the lowest energy score of -801.0 for Cluster 0 highlight a highly favorable and stable binding affinity, essential for effective therapeutic targeting. The lowest energy score indicates the most stable conformation of the protein complex, signifying that Cluster 0 (Fig. 6B) can achieve a highly stable interaction with the receptor, which is crucial for the therapeutic efficacy of the fusion protein. In comparison, Cluster 1, with 58 members and a weighted score of -676.0, and Cluster 2, with 53 members, also show strong interactions with a weighted score of -815 and a lowest energy of -833. A more negative docking score indicates a higher likelihood of binding, while a higher cluster number enhances confidence in the binding model. Despite the favorable scores of Cluster 2, the significantly lower member count reduces its reliability. Clusters 3 to 10 have progressively fewer members and varying energy scores, which, while sometimes favorable, do not match the reliability of Cluster 0 due to their lower frequency of occurrence. The selection of Cluster 0 is further justified by the balance between a high member count and excellent energy scores, highlighting its potential as the most stable and

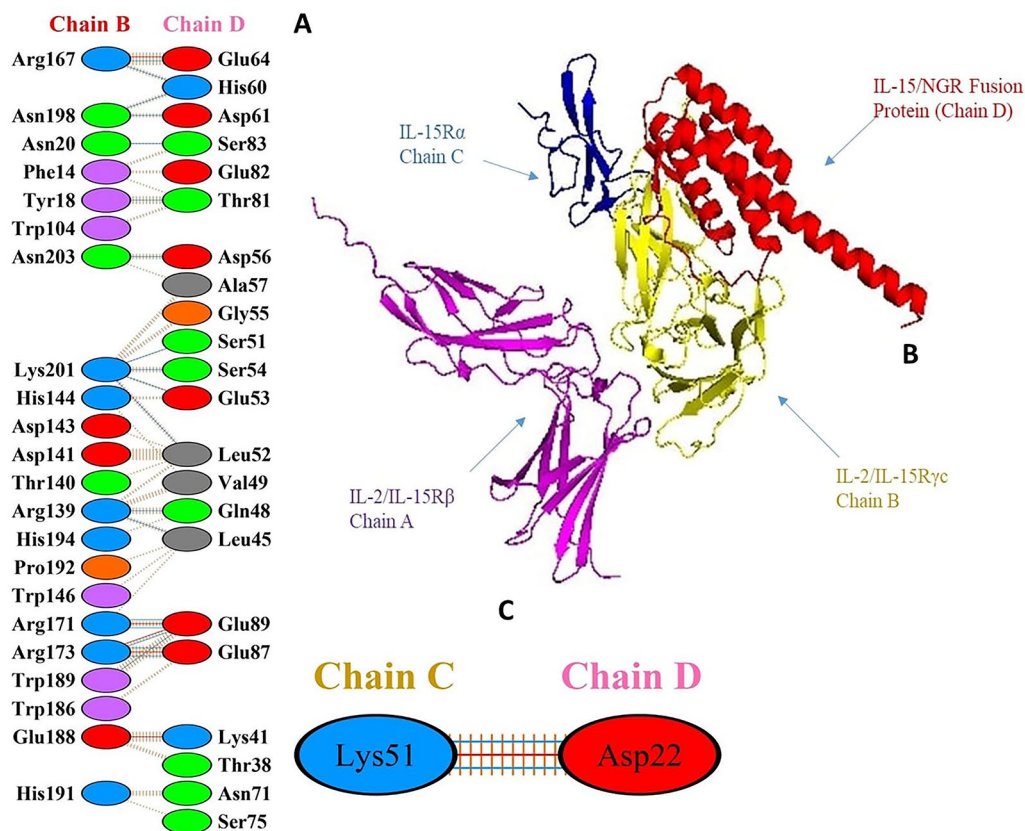


Fig. 6 Docked complex and interacting residues involved hydrogen bonds (blue lines), salt bridges (red line) and disulphide bonds (yellow lines), in binding of IL15-NGR fusion peptide with its cognate receptor

Table 5 Top 10 docked models summary on Hdock server

Sr. #	Docked complex	Docking score	Confidence score	Ligand rmsd (Å)
1	Model 1	-245.18	0.8703	39.69
2	Model 2	-243.35	0.8661	52.41
3	Model 3	-236.63	0.8497	41.33
4	Model 4	-229.94	0.8319	48.83
5	Model 5	-223.81	0.8140	53.14
6	Model 6	-222.37	0.8096	41.11
7	Model 7	-219.95	0.8020	45.53
8	Model 8	-219.70	0.8012	26.01
9	Model 9	-218.76	0.7982	41.13
10	Model 10	-217.88	0.7954	33.67

reproducible interaction between the fusion protein and the IL-15Rα/IL-15Rβ/γc receptor.

The docking of the IL-15-NGR fusion protein with the IL15Rα/IL15Rβ/γc receptor using Hdock yielded notable results. The top ten models displayed docking scores ranging from -245.18 to -217.88 (Table 5), with the highest confidence score being 0.8703. These negative docking scores suggest favorable binding interactions between the fusion protein and the receptor. The ligand

RMSD values ranged from 26.01 Å to 53.14 Å, indicating variability in the predicted binding poses and suggesting flexibility in the interaction sites. The ProQ quality assessment of the input models showed an LGscore of 2.288 and a MaxSub score of 0.205 for the receptor, and an LGscore of 2.944 and a MaxSub score of 0.341 for the ligand. These scores fall into the “good” to “very good” range, indicating that the structural models used for docking were of high quality. The selection of ClusPro-generated docked model was based on binding energy, the number of interactions, and the stability of the docked complex. These factors made the ClusPro generated complex superior, prompting its selection for further interaction analysis and molecular dynamics simulation studies.

Protein-protein interaction studies

Estimating the theoretical binding energies among amino acid residues at protein-protein interfaces presents a challenging task. With advancements in bioinformatics computations, a variety of software and online servers are now available, employing empirical and analytical approaches. However, it’s important to note that results from each module may vary, influenced by the submitted 3D structure of the protein under investigation

(Lubkowski et al. 2018). We utilized the PDBsum program to gain insights into the docked complexes and analyze the forces of attraction at the molecular level. The PDBsum server facilitated the analysis of interactions within the docked complex. The PDB file of the docked complex was submitted to the PDBsum online server for analysis. The length of the interface area and the number of residues therein determine the strength of binding; a higher percentage of amino acids with a longer interface area indicates greater binding strength and a stable conformation (Khan et al. 2021). In the docked complex, a total of 21 hydrogen bonds and 6 salt bridges were identified (Table 6). In the Fig. 6A and B, C, chain D represents the newly designed fusion peptide, chain A represents the IL-2/IL-15R β receptor subunit, chain C represents the IL-15R α receptor subunit, and chain B represents the IL-2/IL-15 γ c receptor subunit. Between chain D and chain B, hydrogen bonds of chain D are contributed by Glu⁶⁴, His⁶⁰, Asp⁶¹, Ser⁸³, Thr⁸¹, Asp⁵⁶, Ser⁵¹, Ser⁵⁴, Glu⁵³, Leu⁵², Gln⁴⁸, Leu⁴⁵, Glu⁸⁹, and Glu⁸⁷. Hydrogen bonds of chain B are contributed by Arg¹⁶⁷, Asn¹⁹⁸, Asn²⁰, Tyr¹⁸, Asn²⁰³, Lys²⁰¹, Arg¹⁹³, Arg¹⁷¹, Arg¹⁷³, and Trp¹⁸⁹. Additionally, hydrogen bonds of chain D are contributed by Asp²², while the hydrogen bond of chain C is contributed by Lys⁵¹. Furthermore, between chain D and chain B, salt bridges of chain D are contributed by Glu⁶⁴, Glu⁸⁹, Glu⁸⁷, and Lys⁴¹, while salt bridges of chain B are contributed by Arg¹⁶⁷, Arg¹⁷¹, Arg¹⁷³, and Glu¹⁸⁸. These hydrogen bonds and salt bridges play central roles in stabilizing the interaction between the fusion peptide and the receptor subunits, providing insights into the molecular mechanisms underlying their binding affinity. The binding energy calculation of the IL-15-NGR fusion protein with the IL15R α /IL15R β / γ c receptor, as predicted using the HawkDock online server, is -2.98 kcal/mol. This negative binding energy indicates a favorable interaction between the fusion protein and the receptor, suggesting that the IL-15-NGR fusion protein can effectively bind to the IL15R α /IL15R β / γ c receptor. The magnitude of the binding energy, while modest, supports the stability of the complex formed. This binding energy is crucial for the therapeutic potential of the fusion protein, as it underlines its ability to target and engage the receptor with sufficient affinity. However, while computational predictions provide valuable insights, these results should be further validated through experimental binding assays to confirm the interaction strength and to refine the binding

efficiency. Finally the results of binding affinity prediction on PRODIGY server suggest that the IL-15/NGR fusion protein binds to its receptor with high affinity at 37 °C. The strongly negative ΔG value of -12.6 kcal mol⁻¹ and the low K_d (constant of dissociation) of 1.2e-09 M, both indicate a strong and stable interaction, suggesting that the fusion protein is likely to effectively engage its receptor under physiological conditions.

MD simulation analysis

Molecular Dynamics (MD) simulations are performed to refine docking results by allowing for conformational flexibility and dynamic adjustments. It helps to assess the stability of the complex over time, investigate key binding interactions, and observe conformational changes that affect binding affinity. The graph in Fig. 7A depicts the radius of gyration (R_g) of a docked complex over a 100-nanosecond (ns) simulation period, indicating changes in the compactness of the molecular structure. Initially, from 0 to 20 ns, the R_g increases from approximately 3.1 nm to around 3.3 nm, suggesting an initial expansion of the complex. Between 20 and 60 ns, the R_g continues to rise and fluctuates around 3.4 nm, indicating further expansion and structural adjustments within the complex. In the later phase, from 60 to 100 ns, the R_g stabilizes and fluctuates between 3.2 nm and 3.4 nm, reflecting a balance between expansion and contraction as the complex reaches a more equilibrated state. These observations suggest that the complex undergoes significant initial conformational changes and expansion, followed by a period of relative stability with minor fluctuations in its compactness, indicative of the complex's dynamic adaptation and stabilization during the simulation. The Fig. 7B illustrates the Root Mean Square Deviation (RMSD) of molecular system over a simulation period of 100 nanoseconds (ns), depicting the structural changes relative to the initial configuration. Initially, from 0 to 20 ns, the RMSD increases sharply from close to 0 to about 0.8 nm, indicating significant structural adjustments as the system moves away from its starting conformation. Between 20 and 60 ns, the RMSD continues to rise but at a slower rate, suggesting ongoing but less dramatic changes in the structure. In the final phase, from 60 to 100 ns, the RMSD stabilizes, fluctuating around 1.0 to 1.2 nm, which signifies that the system has reached a more equilibrated state with only minor fluctuations. This trend reflects the typical behavior in MD simulation

Table 6 Interface statistics of chain A, B, C, D

Chains	IA	IR	SB	DS	HB	NBC
B:D	1019:1014	22:22	–	–	19	127
C:D	42:34	1:1	1	–	2	4
A:B	574:553	11:10	–	–	3	90
B:C	757:922	26:20	3	–	14	491

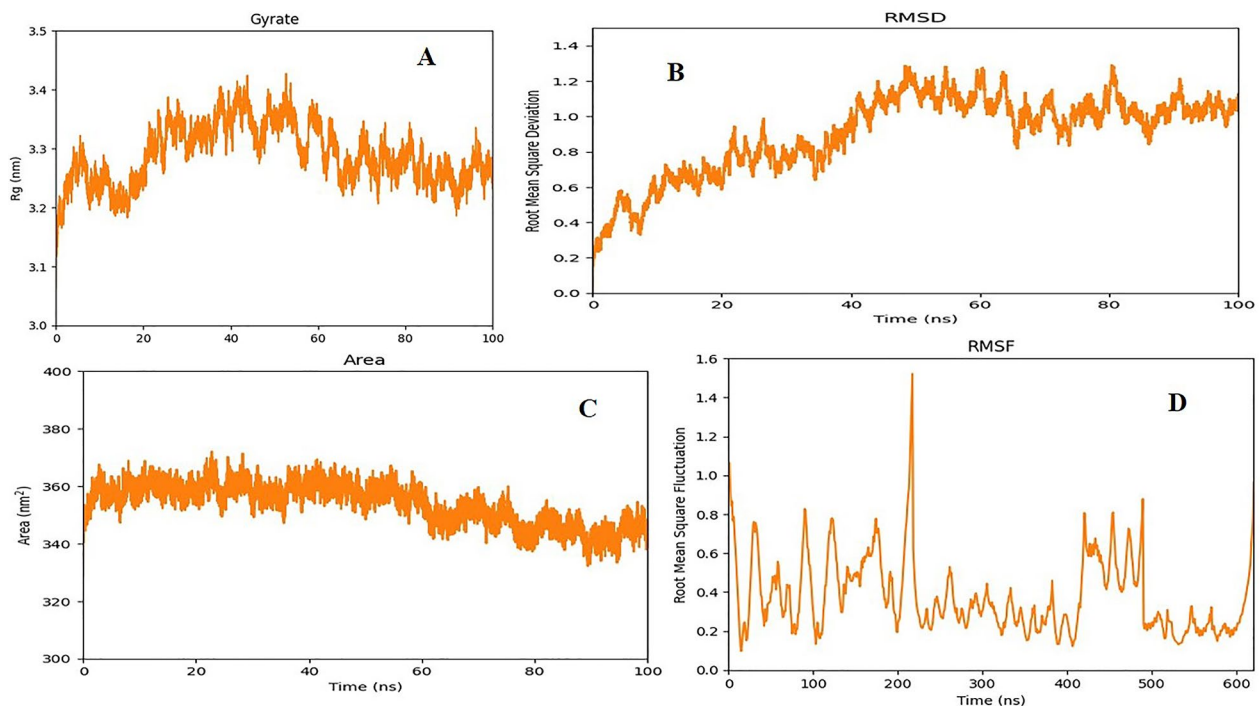


Fig. 7 MD simulation graphs of RMSD, Rg, RMSF and SASA generated by GROMACS for IL15-NGR fusion peptide

where system undergoes an initial period of rapid structural changes before settling into a stable conformation. The graph in Fig. 7C illustrates the area of the interaction interface (in nm^2) between two molecules over time (ns). Initially, during the first 20 ns, the interface area fluctuates between approximately 350 and 370 nm^2 , indicating that the complex is undergoing initial adjustments and conformational changes to find a more stable binding orientation. From 20 to 60 ns, the interface area shows a slight downward trend, fluctuating around 350 to 360 nm^2 , suggesting that the complex is becoming more stable as the interacting surfaces of the molecules adjust to form a tighter interface. In the final phase of the simulation, from 60 to 100 ns, the interface area continues to decrease slightly, with fluctuations between 330 and 350 nm^2 , indicating that the complex is reaching a more stable conformation. The overall decrease in the interface area over time suggests that the molecules are coming closer together, enhancing their interactions, while the fluctuations highlight the dynamic nature of the molecular interactions. The graph in Fig. 7D illustrates the Root Mean Square Fluctuation (RMSF) of a docked complex over a 600-nanosecond (ns) simulation period, providing insights into the flexibility of different regions within the complex. Initially, from 0 to 100 ns, the RMSF values show significant fluctuations, reaching up to approximately 0.8 nm, indicating that certain regions of the complex exhibit considerable movement. In the middle phase, between 100 and 400 ns, the RMSF values display

periodic peaks and troughs, with a pronounced spike around 200 ns where the RMSF peaks at about 1.4 nm, suggesting that specific regions of the complex experience increased flexibility, possibly due to conformational adjustments or interactions with the receptor. In the later phase, from 400 to 600 ns, the RMSF values generally remain below 0.6 nm with occasional fluctuations, except for a notable increase towards the end, peaking again around 1.4 nm, indicating that while most regions of the complex remain relatively stable, certain areas experience heightened flexibility. These observations suggest that the docked complex undergoes dynamic structural changes, with specific regions exhibiting significant flexibility, reflecting its interaction and adaptation processes during the simulation. The MD simulation results indicate that the docked complex undergoes significant conformational adjustments initially, achieving greater stability over time. Overall, these observations reflect the complex's dynamic adaptation and eventual stabilization during the simulation.

Discussion

Hepatocellular carcinoma, the most prevalent primary liver cancer, contributes to up to 1 million fatalities annually worldwide (Befeler and Di Bisceglie 2002). While various treatment modalities exist for hepatocellular carcinoma, including chemotherapy, the emergence of drug resistance necessitates the exploration of novel therapeutic approaches. Ongoing clinical cancer research

emphasizes cytokine therapy's significant role in stimulating the immune system of cancer patients, offering promise as an adjunct or alternative treatment strategy to combat drug resistance and improve outcomes in hepatocellular carcinoma management (Hafiz Muhammad et al. 2024). The discovery that elevated IL-15 levels in peritumoral liver cells correlate with improved prognosis in patients with hepatocellular carcinoma supports the idea of targeting the IL-15 pathway for liver cancer treatment (Zhou et al. 2010). IL-15 exhibits no harmful side effects in vivo, such as the proliferation of T regulatory cells or T-cell activation-induced cell death (Waldmann 2006). In mouse models using recombinant IL-15 (Munger et al. 1995) (Tang et al. 2008), antibody-IL-15 fusion protein (Kaspar et al. 2007), IL-15 gene-modified tumor cells (Kimura et al. 1999) (Meazza et al. 2000), and IL-15 transgenic mice the anticancer potential of IL-15 was reported. Despite advancements in identifying new oncological treatments, the selectivity and efficacy of cancer treatment remain significant barriers. While progress has been made in discovering novel oncological medicines, challenges persist in achieving optimal selectivity and effectiveness. NGR peptide, functioning as a tumor homing peptide, works by internalizing into tumors and blood vessels within the tumor parenchyma, offering promise in addressing these challenges. In the current study, human IL15 was computationally fused with the tumor homing peptide NGR to construct a fusion protein with potential efficacy in treating hepatocellular carcinoma. Tertiary structure prediction, crucial for protein functionality, was performed using two bioinformatics tools: ITASSER and trRosetta. Given the critical importance of properly folded proteins in the human body, accurate prediction of 3D structure is essential. Comparison of models generated by ITASSER and trRosetta revealed that the model predicted by trRosetta exhibited greater stability and accuracy, suggesting its suitability for further analysis and potential therapeutic application. The selected 3D model underwent refinement using the GalaxyRefine web server, renowned for its authenticity in refining tertiary structures. The refinement process involved side chain rebuilding and repacking. Subsequently, to assess the stereochemical quality of the protein structure, the PROCHECK server was employed, which analyzes residue-by-residue geometry and geometry of overall structure to ensure structural integrity and reliability. Ramachandran plot analysis conducted by PROCHECK revealed that the IL15-NGR model contains 99 residues within the most favored region. This indicates that the modeled structure exhibits highly favorable conformational characteristics, affirming its reliability and potential efficacy (Laskowski et al. 1993). The overall quality factor of fusion protein was predicted as 96.72% by ERRAT2 server and the fusion protein was predicted to be stable

on the basis of presence of high alpha helix residues in secondary structure (Sakurai et al. 2005). The physiochemical properties of the fusion protein were assessed using the ProtParam tool, revealing its acidic nature with a molecular weight of 16 kDa. Its predicted isoelectric point of 5.00 is indicative of its solubility characteristics. In silico analysis of soluble protein expression in *E. coli* was conducted using the SoluProt website, yielding a value of 0.844 predicted its high level expression. Protein-protein interactions play a crucial role in various signaling pathways, providing insights into disease mechanisms and aiding in the evaluation of treatment strategies tailored to specific diseases. (De Las Rivas and Fontanillo 2010) described the protein-protein interactions as physical contacts through molecular docking between proteins, which occur within a cell or living organism in vivo. The primary mode of action of IL-15 involves trans-presentation of IL-15 α by dendritic cells and activated monocytes to heterodimer receptor chains (IL-2R/IL-15R β and γ) on effector B, T, and natural killer cells (Dubois et al. 2002). To investigate the interaction between the fusion protein and the selected receptor IL15R $\alpha\beta\gamma$, the Cluspro and Hdock online servers were utilized. Our docking analysis has identified a stable and energetically favorable complex between the fusion protein (IL15-NGR) and the IL15R $\alpha\beta\gamma$ receptor. The selected model on ClusPro, characterized by a low docking energy score of -801.0 , suggests a high likelihood of binding between the fusion protein and the receptor. When compared with Hdock, the ClusPro docking results are more robust and reliable. Cluster 0, with 189 members, exhibited the most favorable interaction model with a weighted score of -617.2 and the lowest energy score of -801.0 , indicating a highly stable and strong binding affinity. The higher number of members in Cluster 0 enhances the confidence in the binding model, compared to the top model in Hdock, which had fewer structural variations. While Hdock provided a good initial validation, the ClusPro results demonstrate a superior and more stable interaction model. The consistent and lower energy scores from ClusPro reinforce the reliability of the docking predictions. The graphs of MD simulation such as RMSD shows significant structural changes in a docked complex with its receptor, with an initial rapid increase followed by stabilization, indicating the complex's adaptation and stabilization. The RMSF graph reveals varying flexibility in different regions, with significant fluctuations initially and during specific intervals, reflecting dynamic interactions and conformational changes. The radius of gyration (Rg) graph indicates initial expansion followed by stabilization, suggesting changes in the compactness and eventual equilibrium of the complex. The graph illustrating the interaction interface area over time shows initial fluctuations and gradual stabilization, indicating closer

molecular interactions and a tighter interface. The MD simulation of the docked complex indicates significant initial structural and conformational changes, with the complex achieving greater stability over time. The interaction interface area decreases, hydrogen bonds increase, and the system stabilizes, reflecting the dynamic nature of molecular interactions and the progression towards a stable binding state. While our computational approach to engineering the IL-15-NGR fusion protein is promising, it has limitations such as the accuracy of structural modeling and inherent uncertainties in docking and simulation setups. To address these, we propose future experimental validation, including in vitro studies on hepatocellular carcinoma cell lines to assess anticancer efficacy, selectivity, and safety, followed by in vivo studies in animal models to evaluate pharmacokinetics, bio-distribution, and therapeutic efficacy. These steps will confirm the protein's potential and guide further optimization for clinical use.

In conclusion, our study presents a comprehensive computational approach to design and evaluate a novel therapeutic strategy for hepatocellular carcinoma. By fusing human IL15 with NGR peptide, we aimed to enhance the selectivity and efficacy of cancer treatment. Through structural modeling, refinement, and protein-protein interaction studies, we successfully identified a stable complex between the fusion protein and the IL15R $\alpha\beta$ receptor, suggesting promising therapeutic potential. These findings emphasize the importance of computational methods in drug discovery and provide a foundation for further experimental validation of the fusion protein's efficacy and safety in preclinical and clinical settings. Overall, our study contributes to the ongoing efforts to develop innovative treatments for hepatocellular carcinoma and other cancers.

Acknowledgments

Authors also extend their appreciation to researchers supporting project Number (RSPD2023R885) at King Saud University Riyadh Saudi Arabia for funding this research.

Author contributions

Formal analysis: TF. Methodology: MMM. Validation: MK, SK. data curation: SN investigation resources: ARA, draft preparation: HB and critical revision of manuscript: HMR.

Funding

This work received funding support from the HEC Pakistan through NRPDU 2021 (Project No. 16935) and the University of the Punjab, Lahore, Pakistan.

Data availability

Data is accessible upon inquiry from Dr. Hamid Bashir via Email: hamid.camb@pu.edu.pk.

Declarations

Conflict of interest

No conflicts of interest declared.

Author details

¹Centre for Applied Molecular Biology (CAMB), University of the Punjab, 87-West canal, Bank Road, Lahore 53700, Pakistan

²Department of Information Technology, University of the Punjab, Lahore, Pakistan

³University Institute of Medical Lab Technology, Faculty of Allied health sciences, The University of Lahore, Lahore 54590, Pakistan

⁴School of Biotechnology, IFTM University, Moradabad 244102, India

⁵Department of Pharmacognosy, College of Pharmacy, King Saud University, Riyadh 11451, Saudi Arabia

Received: 30 May 2024 / Accepted: 25 July 2024

Published online: 07 August 2024

References

- Alpdogan Ö, van den Brink MR (2005) IL-7 and IL-15: therapeutic cytokines for immunodeficiency. *Trends Immunol* 26(1):56–64. <https://doi.org/10.1016/j.it.2004.11.005>
- Arap W, Pasqualini R, Ruoslahti E (1998) Cancer treatment by targeted drug delivery to tumor vasculature in a mouse model. *Science* 279(5349):377–380. <https://doi.org/10.1126/science.279.5349.377>
- Aslam S, Rehman HM, Sarwar MZ, Ahmad A, Ahmed N, Amirzada MI, Rehman HM, Yasmin H, Nadeem T, Bashir H (2023) Computational modeling, high-level Soluble expression and in Vitro cytotoxicity Assessment of recombinant *Pseudomonas aeruginosa* Azurin: a promising anti-cancer therapeutic candidate. *Pharmaceutics* 15(7):1825. <https://doi.org/10.3390/pharmaceutics15071825>
- Befeler AS, Di Bisceglie AM (2002) Hepatocellular carcinoma: diagnosis and treatment. *Gastroenterology* 122(6):1609–1619. <https://doi.org/10.1053/gast.2002.33677>
- Breous E, Thimme R (2011) Potential of immunotherapy for hepatocellular carcinoma. *J Hepatol* 54(4):830–834. <https://doi.org/10.1016/j.jhep.2010.11.022>
- Burton JD, Bamford RN, Peters C, Grant AJ, Kurys G, Goldman CK, Brennan J, Roessler E, Waldmann TA (1994) A lymphokine, provisionally designated interleukin T and produced by a human adult T-cell leukemia line, stimulates T-cell proliferation and the induction of lymphokine-activated killer cells. *Proceedings of the National Academy of Sciences* 91(11):4935–4939. <https://doi.org/10.1073/pnas.91.11.4935>
- Chen F, Liu H, Sun H, Pan P, Li Y, Li D, Hou T (2016) Assessing the performance of the MM/PBSA and MM/GBSA methods. 6. Capability to predict protein–protein binding free energies and re-rank binding poses generated by protein–protein docking. *Phys Chem Chem Phys* 18(32):22129–22139. <https://doi.org/10.1039/C6CP03670H>
- Cheng L, Du X, Wang Z, Ju J, Jia M, Huang Q, Xing Q, Xu M, Tan Y, Liu M (2014) Hyper-IL-15 suppresses metastatic and autochthonous liver cancer by promoting tumour-specific CD8+ T cell responses. *J Hepatol* 61(6):1297–1303. <https://doi.org/10.1016/j.jhep.2014.07.004>
- De Las Rivas J, Fontanillo C (2010) Protein–protein interactions essentials: key concepts to building and analyzing interactome networks. *PLoS Comput Biol* 6(6):e1000807. <https://doi.org/10.1371/journal.pcbi.1000807>
- de Lope CR, Reig ME, Darnell A, Forner A (2012) Approach of the patient with a liver mass. *Frontline Gastroenterol* 3(4):252–262. [https://doi.org/10.1016/S1074-7613\(02\)00429-X](https://doi.org/10.1016/S1074-7613(02)00429-X)
- Decot V, Voillard L, Latger-Cannard V, Aissi-Rothé L, Perrier P, Stoltz JF, Bensoussan D (2010) Natural-killer cell amplification for adoptive leukemia relapse immunotherapy: comparison of three cytokines, IL-2, IL-15, or IL-7 and impact on NKG2D, KIR2DL1, and KIR2DL2 expression. *Exp Hematol* 38(5):351–362. <https://doi.org/10.1016/j.exphem.2010.02.006>
- Dubois S, Mariner J, Waldmann TA, Tagaya Y (2002) IL-15Ra recycles and presents IL-15 in trans to neighboring cells. *Immunity* 17(5):537–547. [https://doi.org/10.1016/S1074-7613\(02\)00429-X](https://doi.org/10.1016/S1074-7613(02)00429-X)
- Gasteiger E, Hoogland C, Gattiker A, Duvaud Se, Wilkins MR, Appel RD, Bairoch A (2005) Protein identification and analysis tools on the ExPASy server. Springer. <https://doi.org/10.1385/1-59259-890-0:571>
- Ghomi FA, Kittilä T, Welner DH (2020) A benchmark of protein solubility prediction methods on UDP-dependent glycosyltransferases. *BioRxiv*. <https://doi.org/10.1101/2020.02.28.962894>
- Giri JG, Kumaki S, Ahdieh M, Friend DJ, Loomis A, Shanebeck K, DuBose R, Cosman D, Park L, Anderson D (1995) Identification and cloning of a novel IL-15 binding protein that is structurally related to the alpha chain of the IL-2 receptor.

- EMBO J 14(15):3654–3663. <https://doi.org/10.1002/j.1460-2075.1995.tb07366.x>
- Golo V, Shaïtan K (2002) Dynamic attractor for the Berendsen thermostat and the slow dynamics of biomacromolecules. *Biofizika* 47(4):611–617
- Grabstein KH, Eisenman J, Shanebeck K, Rauch C, Srinivasan S, Fung V, Beers C, Richardson J, Schoenborn MA, Ahdieh M (1994) Cloning of a T cell growth factor that interacts with the β chain of the interleukin-2 receptor. *Science* 264(5161):965–968. <https://doi.org/10.1126/science.8178155>
- Hafiz Muhammad R, Wardah S, Muhammad Naveed K, Numan Y, Fareeha B, Hamid B, Qurban A, Shiming H (2024) A Comprehensive *In Silico* Study of the NDB-IL-24 Fusion protein for Tumor Targeting: a promising anti-cancer therapeutic candidate. *J Biol Regul Homeost Agents* 38(4):3449–3461. <https://doi.org/10.23812/j.biol.regul.homeost.agents.20243804.274>
- Hebditch M, Carballo-Amador MA, Charonis S, Curtis R, Warwicker J (2017) Protein-Sol: a web tool for predicting protein solubility from sequence. *Bioinformatics* 33(19):3098–3100. <https://doi.org/10.1093/bioinformatics/btx345>
- Helal MA, Shouman S, Abdelwaly A, Elmehraath AO, Essawy M, Sayed SM, Saleh AH, El-Badri N (2022) Molecular basis of the potential interaction of SARS-CoV-2 spike protein to CD147 in COVID-19 associated-lymphopenia. *J Biomol Struct Dynamics* 40(3):1109–1119. <https://doi.org/10.1080/07391102.2020.1822208>
- Hon J, Marusiak M, Martinek T, Kunka A, Zendulka J, Bednar D, Damborsky J (2021) SoluProt: prediction of soluble protein expression in *Escherichia coli*. *Bioinformatics* 37(1):23–28. <https://doi.org/10.1093/bioinformatics/btaa582>
- Izadi S, Anandakrishnan R, Onufriev AV (2014) Building water models: a different approach. *J Phys Chem Lett* 5(21):3863–3871. <https://doi.org/10.1093/bioinformatics/btaa582>
- Jallow F, Bourlon MT, Cira MK, Duncan K, Eldridge L, Elibe E, Estes T, Frank A, Gravitt P, Llera AS (2022) The 10th Annual Symposium on Global Cancer Research: New models for Global Cancer Research, Training, and control. *JCO Global Oncol* 8(Suppl 1):1. <https://doi.org/10.1200/go.22.00000>
- Kaspar M, Trachsel E, Neri D (2007) The antibody-mediated targeted delivery of interleukin-15 and GM-CSF to the tumor neovasculature inhibits tumor growth and metastasis. *Cancer Res* 67(10):4940–4948. <https://doi.org/10.1200/go.22.00000>
- Khan MT, Zeb MT, Ahsan H, Ahmed A, Ali A, Akhtar K, Malik SI, Cui Z, Ali S, Khan AS (2021) SARS-CoV-2 nucleocapsid and Nsp3 binding: an *in silico* study. *Arch Microbiol* 203:59–66. <https://doi.org/10.1007/s00202-020-00000>
- Kimura K, Nishimura H, Hirose K, Matsuguchi T, Nimura Y, Yoshikai Y (1999) Immunogene therapy of murine fibrosarcoma using IL-15 gene with high translation efficiency. *Eur J Immunol* 29(5):1532–1542
- Kozakov D, Hall DR, Xia B, Porter KA, Padhorny D, Yueh C, Beglov D, Vajda S (2017) The ClusPro web server for protein–protein docking. *Nat Protoc* 12(2):255–278. <https://doi.org/10.1038/nprot.2016.169>
- Laskowski RA (2009) PDBsum new things. *Nucleic acids research*. <https://doi.org/10.1093/nar/gkn860>
- Laskowski RA, MacArthur MW, Moss DS, Thornton JM (1993) PROCHECK: a program to check the stereochemical quality of protein structures. *J Appl Crystallogr* 26(2):283–291. <https://doi.org/10.1107/S0021889892009944>
- Le Grazie M, Biagini MR, Tarocchi M, Polvani S, Galli A (2017) Chemotherapy for hepatocellular carcinoma: the present and the future. *World J Hepatol* 9(21):907. <https://doi.org/10.4254/wj.v9.i21.907>
- Lei H, Cao P, Miao G, Lin Z, Diao Z (2010) Expression and functional characterization of tumor-targeted fusion protein composed of NGR peptide and 15-kDa actin fragment. *Appl Biochem Biotechnol* 162:988–995. <https://doi.org/10.1007/s12010-009-8820-8>
- Leonard WJ, Lin J-X, O'Shea JJ (2019) The γ c family of cytokines: basic biology to therapeutic ramifications. *Immunity* 50(4):832–850. <https://doi.org/10.1016/j.immuni.2019.03.028>
- Liang Q, Shen X, Sun G (2018) Precision medicine: update on diagnosis and therapeutic strategies of hepatocellular carcinoma. *Curr Med Chem* 25(17):1999–2008. <https://doi.org/10.2174/0929867324666171025122713>
- Lubkowski J, Sonmez C, Smirnov SV, Anishkin A, Kottenko SV, Wlodawer A (2018) Crystal structure of the Labile Complex of IL-24 with the Extracellular domains of IL-22R1 and IL-20R2. *J Immunol* 201(7):2082–2093. <https://doi.org/10.4049/jimmunol.1701446>
- Marks-Konczalik J, Dubois S, Losi JM, Sabzevari H, Yamada N, Feigenbaum L, Waldmann TA, Tagaya Y (2000) IL-2-induced activation-induced cell death is inhibited in IL-15 transgenic mice. *Proceedings of the National Academy of Sciences* 97(21):11445–11450. <https://doi.org/10.1073/pnas.200363097>
- Meazza R, Lollini PL, Nanni P, De Giovanni C, Gaggero A, Comes A, Cilli M, Di Carlo E, Ferrini S, Musiani P (2000) Gene transfer of a secretable form of IL-15 in murine adenocarcinoma cells: effects on tumorigenicity, metastatic potential and immune response. *Int J Cancer* 87(4):574–581
- Muhammad Rehman H, Rehman HM, Naveed M, Khan MT, Shabbir MA, Aslam S, Bashir H (2023) *In Silico* Investigation of a chimeric IL24-LK6 Fusion protein as a potent candidate against breast Cancer. *Bioinform Biol Insights* 17:11779322231182560. <https://doi.org/10.1177/11779322231182560>
- Munger W, Dejoy SQ, Jeyaseelan Sr R, Torley LW, Grabstein KH, Eisenmann J, Paxton R, Cox T, Wick MM, Kerwar S (1995) Studies evaluating the antitumor activity and toxicity of interleukin-15, a new T cell growth factor: comparison with interleukin-2. *Cell Immunol* 165(2):289–293. <https://doi.org/10.1006/cimm.1995.1216>
- Negussie AH, Miller JL, Reddy G, Drake SK, Wood BJ, Dreher MR (2010) Synthesis and *in vitro* evaluation of cyclic NGR peptide targeted thermally sensitive liposome. *J Controlled Release* 143(2):265–273. <https://doi.org/10.1016/j.jconrel.2009.12.031>
- Ng CX, Lee SH (2020) The potential use of anticancer peptides (ACPs) in the treatment of hepatocellular carcinoma. *Curr Cancer Drug Targets* 20(3):187–196. <https://doi.org/10.2174/156800961966619111141032>
- Pourhadi M, Jamalzade F, Jahani-Najafabadi A, Shafiee F (2019) Expression, purification, and cytotoxic evaluation of IL24-BR2 fusion protein. *Res Pharm Sci* 14(4):320. <https://doi.org/10.4103/1735-5362.263576>
- REHMAN HM, REHMAN HM, AHMED N, IMRAN M (2023) *In silico* design and evaluation of Novel Cell Targeting Melittin-Interleukin-24 Fusion protein: a potential drug candidate against breast Cancer. *Sains Malaysiana* 52(11):3223–3237. <https://doi.org/10.17576/jsm-2023-5211-13>
- Rezaie E, Bidmeshki Pour A, Amani J, Mahmoodzadeh Hosseini H (2020) Bioinformatics predictions, expression, purification and structural analysis of the PE38KDEL-scf immunotoxin against EPHA2 receptor. *Int J Pept Res Ther* 26:979–996. <https://doi.org/10.1007/s10989-019-09944-5>
- Sakurai Y, Mizuno T, Hiroaki H, Gohda K, Oku J-i, Tanaka T (2005) High thermal stability imparted by a designed tandem Arg-Trp stretch in an alpha-helical coiled coil. *Angew Chem Int Ed Engl* 44(38):6180–6183. <https://doi.org/10.1002/anie.200500806>
- Sen TZ, Jernigan RL, Garnier J, Kloczkowski A (2005) GOR V server for protein secondary structure prediction. *Bioinformatics* 21(11):2787–2788. <https://doi.org/10.1093/bioinformatics/bti408>
- Shourian M, Beltra J-C, Bourdin B, Decaluwe H (2019) Common gamma chain cytokines and CD8 T cells in cancer. *Semin Immunol*. <https://doi.org/10.1016/j.smm.2019.101307>
- Siracusano G, Tagliamonte M, Buonaguro L, Lopalco L (2020) Cell surface proteins in hepatocellular carcinoma: from bench to bedside. *Vaccines* 8(11):41. <https://doi.org/10.3390/vaccines810041>
- Sneller MC, Kopp WC, Engelke KJ, Yovandich JL, Creekmore SP, Waldmann TA, Lane HC (2011) IL-15 administered by continuous infusion to rhesus macaques induces massive expansion of CD8+ T effector memory population in peripheral blood. *Blood J Am Soc Hematol* 118(26):6845–6848. <https://doi.org/10.1182/blood-2011-09-377804>
- Tang F, Zhao L, Jiang Y, Ba D, Cui L, He W (2008) Activity of recombinant human interleukin-15 against tumor recurrence and metastasis in mice. *Cell Mol Immunol* 5(3):189–196. <https://doi.org/10.1038/cmi.2008.24>
- Vangone A, Bonvin AM (2015) Contacts-based prediction of binding affinity in protein–protein complexes. *Elife* 4:e07454. <https://doi.org/10.7554/eLife.07454>
- Vanommeslaeghe K, Hatcher E, Acharya C, Kundu S, Zhong S, Shim J, Darian E, Guvench O, Lopes P, Vorobyov I (2010) CHARMM general force field: a force field for drug-like molecules compatible with the CHARMM all-atom additive biological force fields. *J Comput Chem* 31(4):671–690. <https://doi.org/10.1002/jcc.21367>
- Waldmann TA (2006) The biology of interleukin-2 and interleukin-15: implications for cancer therapy and vaccine design. *Nat Rev Immunol* 6(8):595–601. <https://doi.org/10.1038/nri1901>
- Waldmann TA, Lugli E, Roederer M, Perera LP, Smedley JV, Macallister RP, Goldman CK, Bryant BR, Decker JM, Fleisher TA (2011) Safety (toxicity), pharmacokinetics, immunogenicity, and impact on elements of the normal immune system of recombinant human IL-15 in rhesus macaques. *Blood J Am Soc Hematol* 117(18):4787–4795. <https://doi.org/10.1182/blood-2010-10-311456>
- Wang E, Niu R, Wu Y, Hu H, Y, Cai J (2012) Development of NGR-based anti-cancer agents for targeted therapeutics and imaging. *Anti-Cancer Agents Med Chem (Formerly Curr Med Chemistry-Anti-Cancer Agents)* 12(1):76–86. <https://doi.org/10.2174/187152012798918942>
- Zhang C, Zhang J, Niu J, Zhang J, Tian Z (2008) Interleukin-15 improves cytotoxicity of natural killer cells via up-regulating NKG2D and cytotoxic effector

molecule expression as well as STAT1 and ERK1/2 phosphorylation. *Cytokine* 42(1):128–136. <https://doi.org/10.1016/j.cyto.2008.01.003>

Zhou H, Huang H, Shi J, Zhao Y, Dong Q, Jia H, Liu Y, Ye Q, Sun H, Zhu X (2010) Prognostic value of interleukin 2 and interleukin 15 in peritumoral hepatic tissues for patients with hepatitis B-related hepatocellular carcinoma after curative resection. *Gut* 59(12):1699–1708. <https://doi.org/10.1136/gut.2010.212811>

Zhao HL et al (2008) Increasing the homogeneity, stability and activity of human serum albumin and interferon- α 2b fusion protein by linker engineering. *Protein Expr Purif* 61(1):73–77. <https://doi.org/10.1016/j.pep.2008.04.013>

Publisher's Note

Springer Nature remains neutral with regard to jurisdictional claims in published maps and institutional affiliations.